



PERGAMON

Solid State Communications 114 (2000) 481–486

solid  
state  
communications

www.elsevier.com/locate/ssc

# Superparamagnetism in discontinuous Ni films

A. Frydman<sup>a,b,\*</sup>, T.L. Kirk<sup>a</sup>, R.C. Dynes<sup>a</sup><sup>a</sup>Department of Physics, University of California, La Jolla, San Diego, CA 92093, USA<sup>b</sup>Department of Physics, Bar Ilan University, Ramat Gan 52900, Israel

Received 2 November 1999; received in revised form 8 February 2000; accepted 11 February 2000 by A. Pinczuk

## Abstract

We have studied the magnetoresistance (MR) and magnetization of thin discontinuous films of Ni quench-condensed on an insulating substrate. These films show a crossover from superparamagnetic to ferromagnetic behavior as increasing amounts of Ni are added to the film and the film becomes more continuous. We describe the characteristics of this crossover and compare the MR and the magnetization measurements. © 2000 Elsevier Science Ltd. All rights reserved.

*Keywords:* A. Magnetic films and multilayers; A. Nanostructures; D. Electronic transport

## 1. Introduction

Granular ferromagnets, in which random arrays of magnetic grains are embedded in a non-magnetic matrix, exhibit a variety of interesting phenomena. The case where the non-magnetic substance is a metal has achieved increasing attention over the past decade because the granular structures exhibit giant magnetoresistance (GMR) properties that are comparable to those of magnetic heterostructures. The GMR is a result of spin-dependent scattering at the interface between the magnetic particles and the non-magnetic matrix. Systems in which the non-magnetic material is an insulator show similar qualitative negative magnetoresistance (MR) behavior [1–5]. In the insulating samples the origin of the negative MR has been ascribed to spin-dependent tunneling between grains which have randomly oriented magnetic moments [6]. Applying a magnetic field aligns these moments causing a resistance decrease. The amplitudes of the MR peaks are much smaller than those observed in the metallic cases (reaching only a few percent) but the field sensitivity in units of ohms/tesla is much larger because of the large resistance backgrounds.

The transport properties of the insulating granular films, unlike the metallic ones, are very sensitive to the magnetic-grain concentration. At low concentration the grains are

disconnected and the electrons are localized. The mechanism for electrical conductivity is via hopping between grains; thus the resistance depends exponentially on temperature. As the concentration increases, the system becomes percolative and a continuous path of metallic grains connects the entire sample. The conductivity is then diffusive, leading to weak temperature dependence.

The magnetic properties of such a system can also be expected to depend strongly on concentration. If the grains are small and isolated from each other, they will be in the superparamagnetic regime. Hence, above a characteristic temperature,  $T_B$  (the blocking temperature), the magnetization of the grains will be non-hysteretic. The superparamagnetic transition depends on the grain sizes. For a simplified case of uniaxial grains the relationship between the blocking temperature and the average particle volume,  $V$ , is given by [7]:

$$T_B = \frac{KV}{25k_B} \quad (1)$$

where  $K$  is the anisotropy energy. As the magnetic grain concentration increases, the grains can be expected to connect with each other, thus, the average grain volume increases and the system crosses over to ferromagnetic behavior.

The majority of the experiments on insulating granular ferromagnets were performed on samples in which the magnetic and non-magnetic materials were co-evaporated to achieve various concentrations and different samples were required to study different concentrations. In this

\* Corresponding author. Department of Physics, University of California, La Jolla, San Diego, CA 92093.

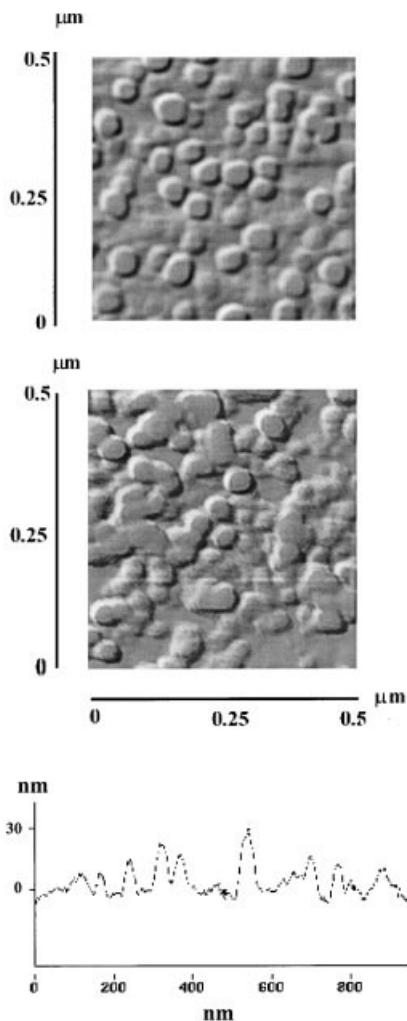


Fig. 1. AFM micrographs of Ni films with nominal thickness of 18 and 23 Å evaporated on a room temperature Si–SiO substrate. Bottom: an AFM line scan of the 18 Å film showing that the average height of the grains is 30 Å.

paper we describe an experiment performed on discontinuous thin Ni films which are granular in nature. The fabrication technique allows us to vary the amount of evaporated Ni in situ, thus enabling us to study the magnetic properties of the film as a function of grain size and inter-grain coupling continuously on the same sample. We observe a transition from non-hysteretic superparamagnetic MR curves to hysteretic ferromagnetic curves as a function of the amount of evaporated material and temperature. The superparamagnetic properties of the grains, as extracted from the MR curves, are found to be very close to those seen in magnetization measurements. However, a quantitative difference is present reflecting the difference in the nature of the measurements.

## 2. Sample fabrication and characterization

The samples described in this work were prepared by “quench-condensation”, i.e. evaporation on a cryo-cooled substrate under UHV conditions within the measurement apparatus using the following scheme. Metallic leads for four-terminal measurements were pre-prepared on an Si–SiO substrate. The substrates were then mounted onto a measurement probe that was immersed in a liquid He bath. The probe was designed so that the sample was situated in an UHV environment and, at the same time, had a good thermal link to the helium bath. We deposited a thin Ni layer using a thermal evaporator placed within the probe while monitoring the film resistance and thickness (using a quartz crystal). The substrate temperature raised during the evaporation but never exceeded 10 K. Once a desired resistance (or film thickness) was achieved we stopped the evaporation and measured the transport and MR curves. We then proceeded to add incremental layers of material in situ and took further measurements at different film resistances. Using this method we were able to study the properties of a single sample as a function of the amount of deposited material while keeping the sample at low temperatures and in UHV environment without having to thermally cycle it (risking metallurgic or structural changes due to annealing) or to expose it to atmosphere (thus oxidizing the Ni surface).

For thin-enough films on a passivated substrate, the Ni layer contains discontinuous grains. The size of these grains is expected to depend upon the substrate temperature. We have performed atomic force microscopic analysis of the morphology of room-temperature-evaporated samples. These are illustrated in Fig. 1. For very thin films the structure contains isolated “pancake-shaped” grain with diameters of a few hundreds of Å and heights of 30–40 Å. As more material is deposited, grains begin to coalesce. The average grain size thus increases and inter-grain spacing decreases until, beyond a percolation threshold, the film becomes continuous.

The grain sizes of quench-condensed samples are expected to be somewhat smaller but the quantitative transition from discontinuous to percolating films is similar. This is realized from the dependence of the resistance on average layer thickness and temperature. Fig. 2 shows that for thickness below  $\approx 23$  Å the resistance drops exponentially with thickness implying that the conduction mechanism is tunneling between grains. For larger thicknesses the film becomes continuous and the resistance crosses over to an ohmic  $1/d$  dependence. A related crossover is observed in the resistance versus temperature curves depicted in Fig. 2. The thinner films exhibit a  $R \propto \exp[T_0/T]^{1/2}$  dependence as expected from hopping between grains [8] (for temperatures above 1 K the  $R$ – $T$  is simply temperature activated:  $R \propto \exp(1/T)$ ). As more material is added we observe a crossover to a  $R \propto \ln(T)$  dependence which implies that the transport is dominated by conduction between the grains hence leading to a weak temperature dependence.

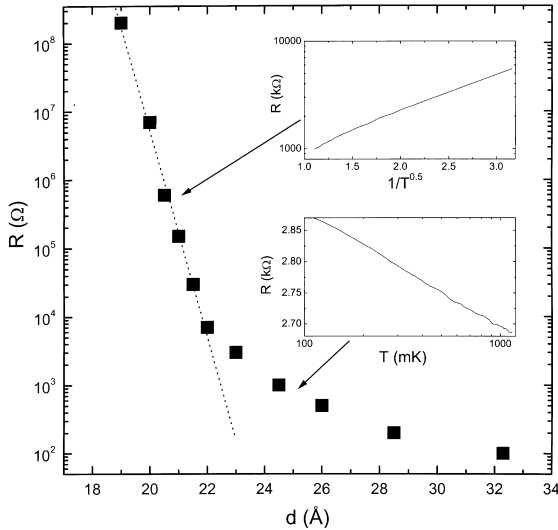


Fig. 2. Sheet resistance versus nominal thickness of a quench-condensed Ni film. The inserts show the temperature dependence for the 21 Å and for the 25 Å stages.

### 3. Magnetoresistance

The MR curves of the granular films also show dramatic changes as ultra-thin layers of material are added to isolated grains. Fig. 3 shows MR curves of a Ni film for different deposition steps. The thinnest film exhibits negative MR centered at  $H = 0$  (Fig. 3a). As more material is deposited a hysteresis develops in the curve, resulting in two resistance peaks at finite magnetic field sweep (depending on the direction of the magnetic field sweep). The position of the peaks shifts towards larger fields as the film thickens (Fig. 3b–f). This behavior can be understood in the following way: for small amounts of material the film consists of small grains which are isolated from each other and are superparamagnetic at  $T = 4$  K. Thus, when the field is removed, the thermal energy is large enough to randomize the spin orientation and the MR curve does not exhibit hysteretic behavior. As more material is deposited, the grains coalesce, the effective magnetic domain sizes become larger, the superparamagnetic blocking temperature rises and the film exhibits ferromagnetic behavior at  $T = 4$  K.

The superparamagnetic nature of the grains manifests itself in the temperature dependence of the hysteresis. We quantify the degree of hysteresis in the system by studying the coercive field,  $H_c$ , for which the magnetization in the system,  $M$ , equals zero. In a granular film this is the field required to totally randomize the magnetic orientations of the different grains, hence it should correlate with the field at which the resistance peaks in the MR. Fig. 4 shows the dependence of  $H_c$  on temperature for different evaporation stages. The curves are fitted with the superparamagnetic

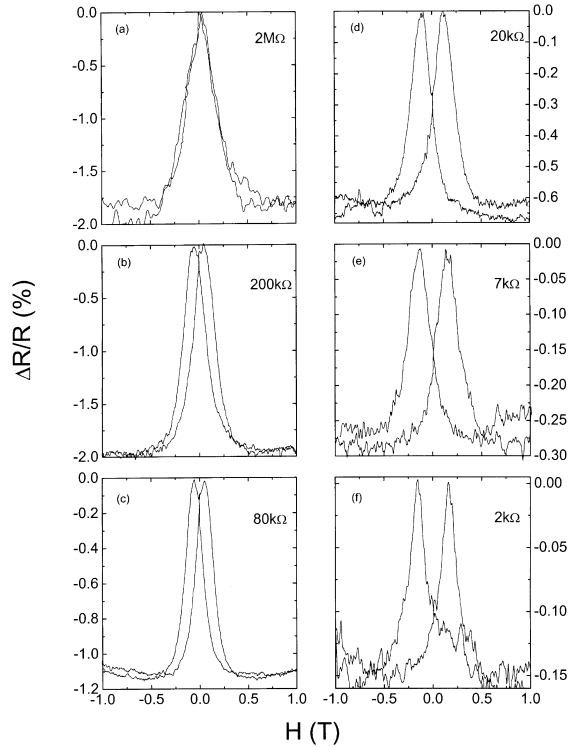


Fig. 3. MR curve at  $T = 4.2$  K of a quench-condensed Ni film for different steps of the evaporation. The field was swept from  $-1T$  to  $1T$  and back. The nominal film thicknesses were: (a) 20; (b) 20.5; (c) 21; (d) 21.8; (e) 23; and (f) 25 Å.

expression:

$$h_c = \frac{H_c}{H_{c0}} = 1 - \left( \frac{T}{T_B} \right)^{1/2} \quad (2)$$

$$H_{c0} = \frac{2K}{M_s} \quad (3)$$

where  $M_s$  is the saturation magnetization. It is seen that as the nominal thickness increases the blocking temperature (for which  $H_c = 0$ ) rises. This is in agreement with the notion that the average grain size increases with adding material due to grain coalescing, which, according to Eq. (1), would result in an increase of  $T_B$ . As will be shown later, the grain diameters grow by an order of 100 Å while the nominal film thickness increases only by several Å.

Another obvious trend can be seen from Fig. 3. As material was added and the sheet resistance was reduced, the amplitude of the MR decreased. Adding an average thickness of 7 Å to the film reduced the resistance by three orders of magnitude and caused  $\Delta R/R$  to drop from 2 to 0.15%. We attribute this to the expanding of equivalent chains in the percolation network for conductivity as material is added.

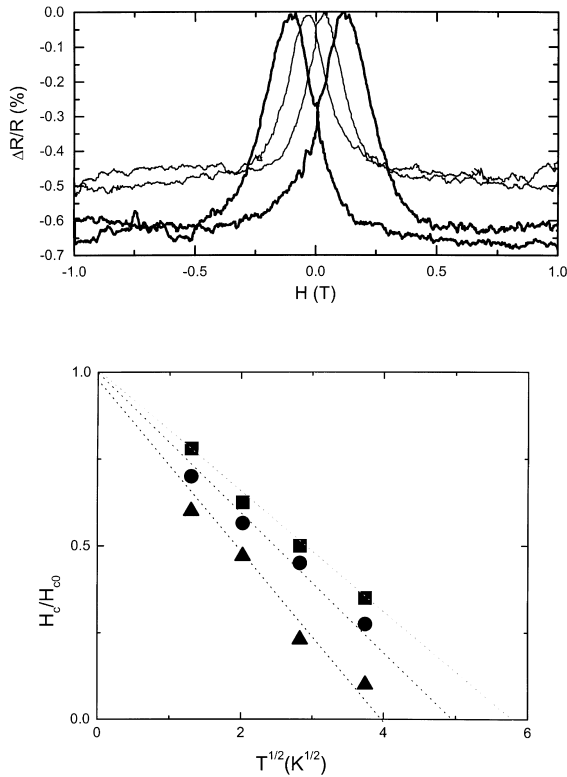


Fig. 4. Top: MR of a 22 Å-thick sample at  $T = 2$  K (heavy solid line) and 10 K (light solid line). Bottom: normalized coercive field as determined from the MR versus temperature for three evaporation stages. The thicknesses and resistances of the samples are: 10 k $\Omega$ , 22 Å (triangles), 3 k $\Omega$ , 24 Å (circles) and 1 k $\Omega$ , 27 Å (squares).

The reduction of the MR amplitude reflects the fact that the number of spin-dependent tunneling processes in the relevant current trajectories is decreasing. In the extreme limit, when  $R$  crosses over to the  $1/d$  dependence, all the grains are connected and there are no spin-dependent tunneling processes. Hence, the negative MR is expected to disappear [9].

#### 4. Magnetization

It is clear that the details of the current trajectories highly effect the amplitude of the MR. The magnetization of the grains, on the other hand, should not depend on the current paths. One is then compelled to ask how well the MR curves describe the magnetization state of the grains. The usual model which is used to describe the relationship between the two entities predicts the following [6]:

$$\frac{\Delta\rho}{\rho} = \left(\frac{JP}{4kT}\right)L^2\left(\frac{\mu H}{kT}\right) \quad (4)$$

for superparamagnetic particles and

$$\frac{\Delta\rho}{\rho} = -\left(\frac{JP}{4kT}\right)[M^2(H, T) - M^2(0, T)] \quad (5)$$

for ferromagnetically coupled particles. Here  $P$  is the polarization of the electrons,  $J$  the exchange coupling within the grain,  $L$  the Langevin function,  $\mu$  the magnetic moment of the grains and  $M$  the magnetization of the films. According to this model, the coercivity measured by MR or directly by magnetization should be equal. We have compared the MR curves of a few of our samples with magnetization versus field measurements ( $M-H$ ) taken in a SQUID magnetometer. For these measurements we coated the discontinuous Ni grains with a 20 Å layer of Ge prior to exposing it to room conditions. This process has been shown to have no effect on the magnetic properties of the film [10]. We found [10] that the values for the coercive field derived from the MR measurements are larger by about 30% than those derived from the magnetization measurements. Such a difference in the measured  $H_c$  is typical for many samples and reflects the conceptual difference between the two types of measurement. While the magnetization curve probes the entire sample, the MR only probes those grains that participate in the percolation network. The discrepancy we detect suggests that the grains that determine the percolation path are larger than the average, thus causing the coercive field to shift to larger values. This is not surprising. One may expect small grains that are more isolated not to contribute to the conduction. Hence, the MR only reflects the magnetic properties of part of the film. Nevertheless, the qualitative behavior exhibited by the MR is reproduced by the measured magnetization. Fig. 5 shows the temperature dependence of the hysteresis loops and the coercive fields. The general trend is very similar to that of Fig. 4, as are the values for the blocking temperatures extracted from these curves.

#### 5. Anisotropy

One of the difficulties when dealing with low-dimensional systems is to determine the type and magnitude of the magnetic anisotropy. Bulk Ni has a magneto-crystalline anisotropy of  $0.5 \times 10^5$  erg/cm<sup>3</sup> in the [111] direction which, for our films, would be directed out of the film plane [11]. Since our samples are thin films and the grains are disk-like shaped with an aspect ratio of about 7, one can expect the shape anisotropy to be rather prominent, giving rise to a  $4\pi M$  in-plane contribution. Another contribution to the anisotropy is the large surface area present in the grains. It has been shown that surface and magneto-elastic considerations cause thin films of Ni on Cu or Si substrates to exhibit a magnetization reorientation transition from in-plane, for ultra-thin films, to out of the plane, for films of 30–150 Å, and back in the plane, for thicker layers [12–16]. In addition to all of the above one must take into consideration the stress anisotropy that may be present in the interface

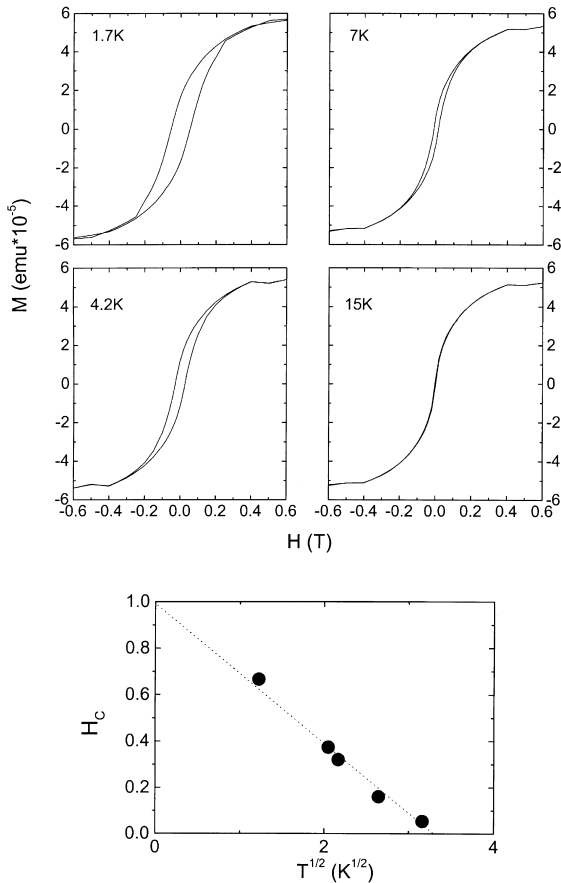


Fig. 5. Magnetization measurements of a 22.5 Å-thick sample at various temperatures. Bottom graph: coercive field, as extracted from the above curves, versus temperature.

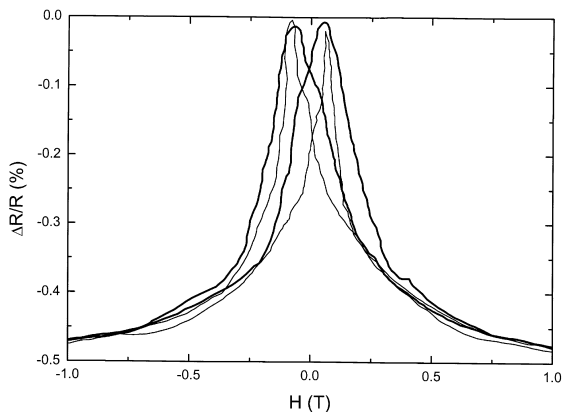


Fig. 6. MR curves of a room-temperature-evaporated film in parallel (light solid) and perpendicular (heavy solid) magnetic fields.  $T = 4$  K.

between the Ni and the SiO<sub>2</sub>. In an attempt to determine the nature of the anisotropy in our films we have compared MR measurements of a specific sample (grown at room temperature) in parallel field versus perpendicular field. The results are shown in Fig. 6. It is seen that the coercivities for the two field orientations are very similar. We therefore speculate that the anisotropy of the grains is a combination of two or more of the above, leading to a comparable coercivity in plane and perpendicular to the plane.

The magnitude of the anisotropy energy can be estimated from the fits of Fig. 5 and Eq. (3). The fitted value for  $H_{c0}$  is  $\approx 1700$  Oe and the measured  $M_s$  (estimated from Fig. 5) is  $250 \text{ emu/cm}^3$ . This yields an anisotropy energy of  $K = 10^5 \text{ erg/cm}^3$ . Inserting this value into Eq. (1) and using the blocking temperatures from Fig. 5 allows us to estimate the average grain volume. The values of the calculated grain diameters,  $D$ , (assuming a uniform height of  $\approx 30$  Å) are given in the following table:

$d$ (Å)	$R$ (kΩ)	$T_B$ (K)	$D$ (Å)
22	10	16	192
24	3	24	236
27	1	34	280

These diameters are somewhat smaller than those of the room-temperature-evaporated samples as seen from the atomic force micro-pictures (Fig. 1) but are reasonable numbers for low- $T$  condensation.

## 6. Summary

The quenched condensed samples we have studied show a crossover from non-hysteretic to hysteretic MR and magnetization curves. This crossover correlates with a transition from hopping to diffusive transport and with the evolution of the film morphology from isolated grains to large clusters. We ascribe this crossover from a superparamagnetic to ferromagnetic transition to an increase in the typical magnetic grain size. Recently we have shown that a similar crossover (though weaker) is present even when non-magnetic material is added to isolated ferromagnetic grains [10]. We interpreted this as being due to magnetic coupling of the grains via the non-magnetic media.

The quench-condensation technique is a promising tool for low-dimensional magnetic studies since it eliminates one of the largest difficulties in this area, i.e. the rapid oxidation of the surfaces. It also provides a very delicate control over the desired parameters. We hope to use the methods described in this work to investigate further relevant issues such as interactions between magnetic nano-particles.

## Acknowledgements

We are grateful for illuminating discussions with A.E. Berkowitz, F. Hellman, S. Sankar and H. Suhl. This research was supported by AFSOR grant no. F49620-92-j-0070.

## References

- [1] J.I. Gittelman, Y. Goldstein, S. Bozowski, Phys. Rev. B 5 (1972) 3609.
- [2] A. Milner, A. Gerber, B. Groisman, M. Karpovsky, A. Gladkikh, Phys. Rev. Lett. 76 (1996) 475.
- [3] W. Yang, Z.S. Jiang, W.N. Wang, Y.W. Du, Solid State Commun. 104 (1997) 479.
- [4] S. Honda, T. Okada, M. Nawate, M. Tokumoto, Phys. Rev. B 56 (1997) 14566.
- [5] S. Sankar, A.E. Berkowitz, Appl. Phys. Lett. 73 (1998) 535.
- [6] J.S. Helman, B. Abeles, Phys. Rev. Lett. 37 (1976) 1429.
- [7] L. Néel, Compt. Rend. 228 (1949) 664.
- [8] P. Sheng, B. Abeles, Y. Arie, Phys. Rev. Lett. 31 (1973) 44.
- [9] A. Frydman, E.P. Price, R.C. Dynes, Solid State Commun. 106 (1998) 705.
- [10] A. Frydman, R.C. Dynes, Solid State Commun. 110 (1999) 485.
- [11] B. Abeles, P. Sheng, M.D. Coutts, Y. Arie, Advances in Physics 24 (1975) 407.
- [12] S.Z. Wu, G.J. Mankey, F. Hung, R.F. Willis, J. Appl. Phys. 76 (1994) 6434.
- [13] B. Schultz, K. Baberschke, Phys. Rev. B 50 (1994) 13467.
- [14] G. Bochi, C.A. Ballentine, H.E. Inglefield, C.V. Thompson, R.C. O'Handley, J. Appl. Phys. 79 (1996) 5845.
- [15] G. Bochi, C.A. Ballentine, H.E. Inglefield, C.V. Thompson, R.C. O'Handley, Phys. Rev. B 53 (1996) 1729.
- [16] W.L. O'Brien, T. Droubay, B.P. Tonner, Phys. Rev. B 54 (1996) 9297.